Available online at www.sciencedirect.com
ScienceDirect
Journal of Sound and Vibration 303 (2007) 239–254
JOURNAL OF SOUND AND VIBRATION
www.elsevier.com/locate/jsvi

Dynamic performance of slender suspension footbridges under eccentric walking dynamic loads

Ming-Hui Huang[a,b], David P. Thambiratnam[a,*], Nimal J. Perera[c]

[a]School of Urban Development, Queensland University of Technology, GPO Box 2434, Brisbane, Queensland 4001, Australia
[b]School of Civil Engineering and Architecture, Nanchang University, Nanchang, Jiangxi 330029, People's Republic of China
[c]Bird & Marshall Ltd., Warwick House, 25 Buckingham Palace Road, London SW1W 0PP, UK

Received 5 May 2006; received in revised form 9 October 2006; accepted 19 January 2007
Available online 26 March 2007

Abstract

This paper treats the vibration of slender suspension footbridges caused by eccentrically distributed walking dynamic loads. A suspension footbridge model with reverse profiled cables in both the vertical and horizontal planes was used in this conceptual study, while SAP2000 package is adopted in the numerical analysis. The dynamic behaviour of slender footbridges under walking dynamic loads is simulated by resonant vibration caused by synchronous excitations. It is found that slender suspension footbridges with shallow cable profiles often have coupled vibration modes such as coupled lateral–torsional or coupled torsional–lateral modes. When these coupled vibration modes are excited by walking pedestrians, excessive lateral vibration can be induced. Results also show that the effects of the reverse profiled cables on the dynamic performance in different vibration modes are complex. Reverse profiled cables in the horizontal plane can significantly suppress the lateral vibration in coupled lateral–torsional modes, but slightly increase the lateral vibration in coupled torsional–lateral modes.

1. Introduction

With the emergence of new materials and advanced engineering technology, modern footbridges can be designed and constructed to have longer spans and greater slenderness than ever to satisfy the transportation needs and the aesthetical requirements of society. Such slender footbridges have often low stiffness, low mass, low damping and are prone to vibration induced by human activities. The decreasing of mass and stiffness in footbridge structures leads to low natural frequencies for footbridges with greater danger of resonance [1] and larger lateral dynamic response [2]. Severe vibration serviceability problems can arise, particularly in the lateral direction as pedestrians are more sensitive to the low-frequency lateral vibration than the vertical one [3]. This phenomenon has been evidenced by the excessive lateral vibrations of many footbridges worldwide

*Corresponding author. Tel.: +61 7 3138 1467; fax: +61 7 3138 1170.
E-mail address: d.thambiratnam@qut.edu.au (D.P. Thambiratnam).

0022-460X/$ - see front matter © 2007 Elsevier Ltd. All rights reserved.
doi:10.1016/j.jsv.2007.01.016

Nomenclature

A_{ustd}	steady dynamic amplitude of lateral deflection
$[C]$	damping matrix
DAF	dynamic amplification factor
DAF_{ustd}	dynamic amplification factor of steady lateral deflection
D_1, D_2, D_3	diameters of top, bottom and side cables
f_n	pacing frequency of normal walk
$F_n[t]$	force function of normal walk
$F_{nl}(t)$	continuous lateral force function
$F_{nv}(t)$	continuous vertical force function
f_p	pacing frequency of walking load
F_1, F_2, F_3	cable sags of top, bottom and side cables
k	integer number
$[K]$	stiffness matrix
L	span length
L	lateral vibration mode
L_mT_n	coupled lateral–torsional modes
m, n	number of half-wave
M	mass density
$[M]$	diagonal mass matrix
M_{ustd}	mean value of lateral deflection
$q_{nv}(t)$	vertical dynamic force
$q_{nl}(t)$	lateral dynamic force
$q_{sv}(t)$	vertical ramped static force
$\{R\}$	vector of applied loads
t	time
T	torsional vibration modes
T_n	period of normal walk
T_{nc}	contact time
T_p	period of walking load
T_mL_n	coupled torsional–lateral modes
T_1, T_2, T_3	tension forces in top, bottom and side cables
U_l, U_v	lateral and vertical deflections
U_{stdmax}	maximum steady dynamic deflection
U_{stdmin}	minimum steady dynamic deflection
U_{static}	static deflection
$\{U\}$	vector of dynamic displacements
$\{\dot{U}\}$	vector of dynamic velocities
$\{\ddot{U}\}$	vector of dynamic accelerations
V_m	vertical modes
α	time factor

such as Millennium Bridge in London [4], T-Bridge in Japan [5], etc. It is generally accepted nowadays that modern slender footbridges have greater danger of suffering vibration serviceability problems rather than safety or strength problems [6].

In general, lateral deflection is considered as a response to lateral loads. However, vertical loads can also induce lateral deflections, particularly in slender structures such as frames and long bridges. This is because structures are three-dimensional (3D) and deflections in all orthogonal directions are often coupled [7]. This always occurs when vertical loads act on asymmetric structures or asymmetrically (eccentrically) distributed vertical loads act on symmetric structures. It is also reported that horizontal movements of some railway bridges in China have been observed due to the increasing speed of trains [8]. As there are often two or more rail tracks on a bridge, the loading from one train is effectively asymmetrical on the structure and hence lateral movements are generated [7]. For slender suspension footbridges, it is found that large lateral deflection can be induced by eccentric vertical loads [9]. This situation could be worse when lateral vibration is caused when pedestrians walk eccentrically across a slender footbridge, as large lateral vibration can easily trigger synchronous lateral excitation.

A conceptual study is undertaken to comprehensively investigate the dynamic characteristics of slender footbridges with shallow cable profiles under human-induced dynamic loads. A slender suspension footbridge model with pre-tensioned reverse profiled cables in vertical plane as well as in horizontal plane is proposed for this purpose. This paper concerns the vibration, particularly in the lateral direction, induced by eccentric walking dynamic loads when pedestrians walk across the footbridge at different pacing frequencies. Three types of bridge models with different cable configurations are considered to investigate the effect of cable configuration. In the numerical analysis, the structural analysis software package SAP2000 [10] is adopted for the non-linear direct-integration time history analysis. The research finding is helpful to understand the dynamic behaviour of slender suspension footbridges with shallow cable profiles under human-induced dynamic loads.

2. Suspension footbridges with reverse profiled cables

2.1. Proposed suspension footbridge model

The proposed suspension footbridge model is shown in Fig. 1. In this bridge model, the cable system is composed of three groups of cables which may have same or different cable profiles: top supporting cables, bottom reverse profiled cables (Fig. 1(a)) and side bi-concave cables (Fig. 1(b)). The top cables are two parallel suspending cables which have catenary profiles and provide tension forces to support the structural gravity loads, applied loads and extra internal forces induced by the bottom cables. Two parallel bottom cables are designed to have reverse profiles in the vertical plane and their function is to provide extra internal vertical forces to transverse bridge frames and the top supporting cables. The side cables are a pair of bi-concave cables which have the same cable profiles in the horizontal plane, and their main function is to provide extra internal horizontal forces and horizontal stiffness. When the bottom and/or side cables are slack, they could carry small tension forces only to support their own gravity loads and cannot resist any external loads. In this case, they will not be able to contribute stiffness and tension forces to the structure. However, these small tensions can provide sufficient restraining forces to prevent the transverse frames from swaying in the longitudinal direction.

Transverse bridge frames are designed to support the deck and hold the cables. These frames (Fig. 1(c)) comprise cross members (for the support beams and deck), top and bottom vertical legs as well as horizontal side legs and they form a set of spreaders for the cables to create the required profiles. They have in-plane stiffness to protect against collapse under in-plane forces and contribute very little in the way of longitudinal, lateral and rotational stiffness for the entire system. The transverse bridge frames are hung from the top cables, and further restrained by the lower reversed profile cables as well as the side cables. Two support beams of rectangular section are simply supported on cross members of the adjacent bridge frames, and the deck units are simply supported at the ends on these beams.

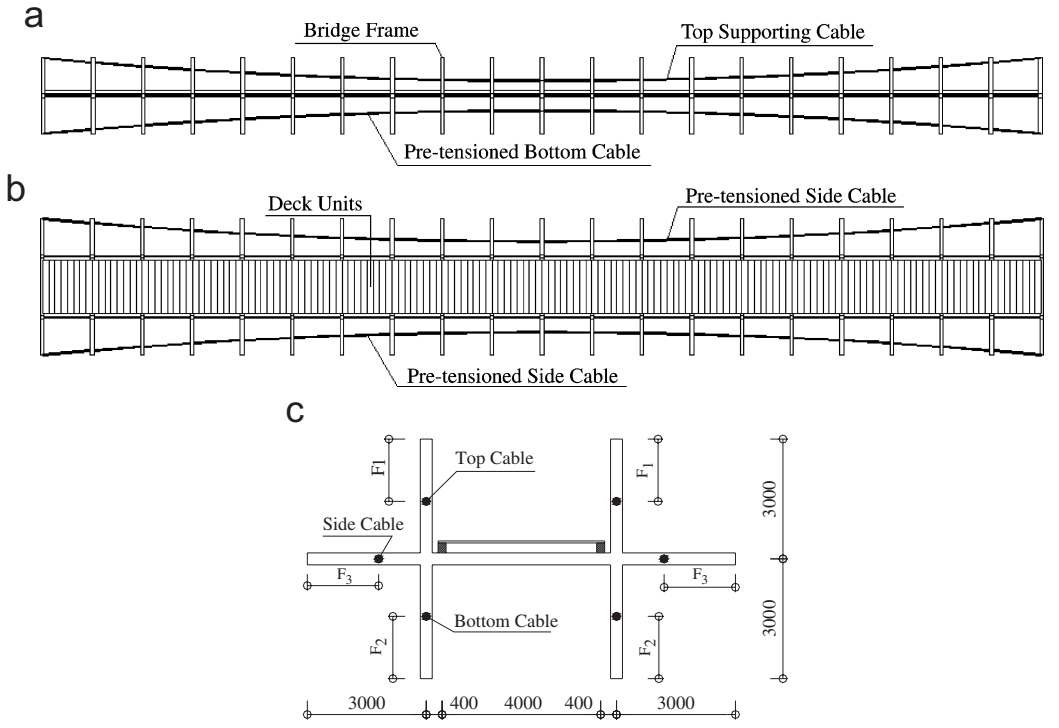

Fig. 1. Suspension footbridge model with reverse profiled cables: (a) elevation; (b) top view; (c) middle transverse bridge frame.

In order to simplify the analysis, all the transverse bridge frames are assumed to have the same size, and hence the weight of frame and deck acting on the cables can be considered as equal concentrated loads. All the cables are stretched by introducing initial distortions to maintain the designed cable sags or cable profiles and required internal forces, and then the decks can be kept in a horizontal plane.

In the bridge model, stainless steel (Young's modulus $2.0 \times 10^{11}\,\mathrm{N/m^2}$ and density $7850\,\mathrm{kg/m^3}$) is chosen for the transverse bridge frames and support beams, and aluminium (Young's modulus $6.5 \times 10^{10}\,\mathrm{N/m^2}$ and density $2700\,\mathrm{kg/m^3}$) is chosen for the deck units. To reduce the weight of the bridge structure, hollow rectangular sections and extruded sections shown in Fig. 2 are used for the members of the transverse bridge frames, support beams and decks. Eight deck units are simply supported on the support beams which span on the cross members of the adjacent transverse bridge frames. Stainless steel cables are chosen for all the cable systems and the material properties are the same as those of bridge frames.

2.2. Finite element modelling and numerical analysis

The structural analysis package SAP2000 is adopted to carry out extensive numerical analyses by using Finite Element method. The proposed footbridge model is modelled as a space frame structure with 3D prismatic beam (cable) elements. A beam (cable) element has two end nodes and each end node has six degrees of freedom: three translations along the local axes and three rotations about its axes. The deflection of the structural model is governed by the displacements of the joints, and different connections, supports and boundary conditions are simulated by applying corresponding end releases and joint restraints.

In the finite element modelling, bridge deck units are assumed to be simply supported by the supporting beams and are modelled as 3D beam elements with end releases: the two ends are supposed to have the same pin connections to the supporting beams and can carry torques and axial forces in order to keep the structure symmetric about the bridge centre line. The supporting beams are also modelled as 3D beam elements with end releases (pin connections), but one end cannot carry torque and axial force. Therefore, the axial force and torque in a supporting beam are only caused by the loads on the supporting beam. For the bridge frame, the members are modelled as 3D beam elements rigidly connected together at the intersection points. All the joints on the bridge frames at the two ends of the bridge model are assumed to have fixed joint restraints (i.e. zero translations and rotations), and therefore these frames will have almost no effect on the structural performance and vibration properties. The cables are modelled as tension only members having large deflections by using beam/frame elements. To simulate the flexible behaviour of cables, each cable element is divided into 20 segments and the moments of inertia of section and torsional constant are modified by a multiplication factor of 0.01. From structural dynamics principles, the governing equations of the footbridge can be developed as [10]

$$[K]\{U(t)\} + [C]\{\dot{U}(t)\} + [M]\{\ddot{U}(t)\} = \{R(t)\}, \tag{1}$$

where $[K]$ is the stiffness matrix; $[C]$ is damping matrix; $[M]$ is the diagonal mass matrix; $\{U(t)\}$, $\{\dot{U}(t)\}$ and $\{\ddot{U}(t)\}$ are the displacements, velocities and accelerations of the structure; and $\{R(t)\}$ is the applied load.

Slender suspension footbridges have large displacements and hence the stiffness matrix is not constant and the effect of axial forces and large deformation should be considered. The entire structural stiffness is mainly provided by the cable system and depends significantly on the cable tensions as well as cable profiles. The

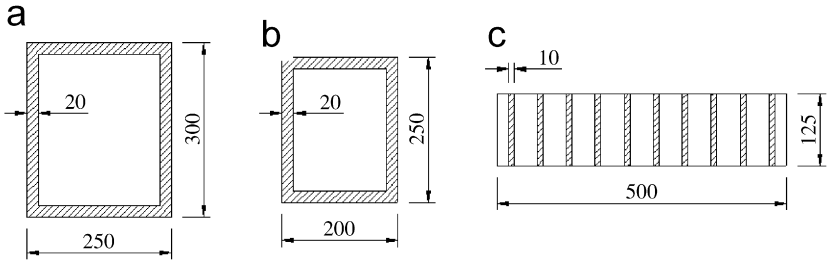

Fig. 2. Sections of bridge members: (a) member of bridge frame; (b) supporting beams; (c) deck units.

tension forces provide load resistances in different directions through the cable profiles and hence affect the stiffness. When a bridge structure deforms or vibrates under applied loads, the cable profiles deform and these changes influence the tension forces and hence affect the structural stiffness as well as the dynamic properties. In general, cables in vertical plane mainly provide force components in vertical and longitudinal directions, and they produce small lateral force components only when they have lateral deformation. On the other hand, lateral stiffness can be considerably improved by cables in horizontal plane [9].

In order to investigate the effects of cable configuration and fundamental natural frequency, three bridge models with different cable configurations are studied in this conceptual study and it is assumed that all the top, bottom and side cables have the same cross section (diameter) and cable sag. Bridge model A—a footbridge model with top supporting cables and pre-tensioned bottom reverse profiled cables, the side cables and side legs of the bridge frames are removed. Bridge model B—a footbridge model with top supporting cables, and pre-tensioned bottom and side cables, and its fundamental natural frequency in lateral direction equals to that of bridge model A. Bridge model C—a bridge model which has the same pretension in reverse profiled bottom cables as bridge model A, but improved by the addition of reverse profiled side cables.

In the following free vibration analysis, the un-damped form of Eq. (1) is used to obtain the natural frequencies and their corresponding vibration modes. The structural stiffness $[K]$ used here is the one when all the cables are stretched to keep the designed cable profiles (or cable sags) and the bridge deck is assumed to be in horizontal plane.

When the suspension footbridge model is subjected to walking dynamic loads, the structural stiffness $[K]$ is affected by the deformation. To obtain the dynamic response, non-linear direct-integration time history analysis is carried out by using Hilber–Hughes–Taylor method. Small time step is used to ensure the accuracy and this time step varies from 0.01 to 0.03 s (less than one fortieth of the period) for walking dynamic load with different pacing frequencies. Since damping in real structures is very complex and structure dependent, proportional damping is used. In this proportional damping model, the damping matrix is assumed to be a linear combination of the stiffness matrix and mass matrix with two defined coefficients [10]. In this conceptual study, these two coefficients are selected according to the periods (or natural frequencies) and it is supposed that both the first and second vibration modes in the same type have the same damping ratio.

3. Walking dynamic loads

It's widely recognized synchronous excitation can be caused by the combination of high density of pedestrians and low natural frequencies of bridges within the frequency range of pacing frequency. When synchronization occurs, footbridges resonate near or at the natural frequency within the frequency range of pacing frequency, and part of pedestrians will change their footfalls to match the vibration. To model the synchronous walking dynamic loads, the following assumptions are adopted:

(i) About 20% of pedestrians participate fully in the synchronization process and generate vertical and lateral dynamic loads at a pacing frequency coinciding with one of the natural frequencies of the footbridge. The remaining 80% pedestrians generate only static vertical load on the bridge deck as they walk with random pacing frequencies and phases.
(ii) The force generated by a footfall has components in the vertical, lateral and longitudinal directions. The vertical component follows the Wheeler's force–time functions [11] and the lateral component has the same force function as its vertical component, but the magnitude is only a small portion (4%) [12] of the vertical component. The longitudinal component is not important for the lateral vibration and is neglected.
(iii) The pedestrian load is uniformly distributed on the whole bridge deck, the load density is set to be 1.5 persons/m^2 and the average weight of a person is 700 N [11].

Fig. 3 shows the typical vertical force functions [11] from slow walk to fast walk. As the force functions are frequency dependent, the walking activities can be classified into four types according to their pacing frequencies and each type of activity covers a range of frequency and have the similar force function but

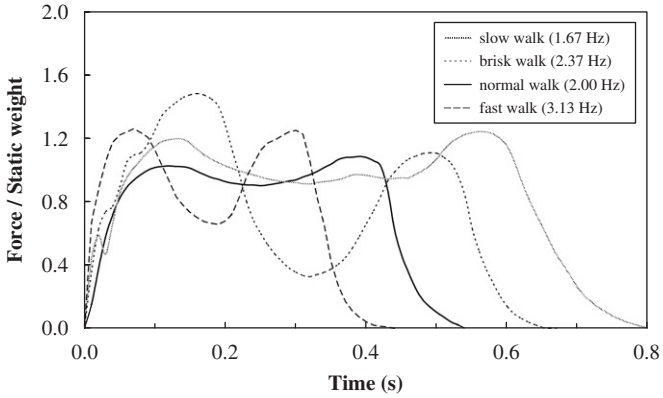

Fig. 3. Typical vertical force patterns of walk activities.

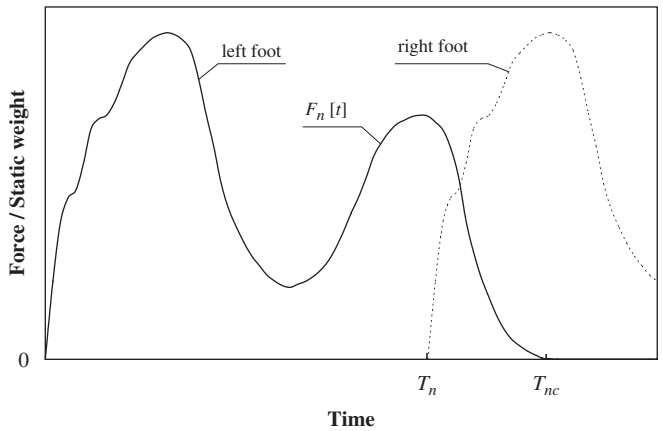

Fig. 4. Force function of normal walk.

different pacing frequency: slow walk (less than 1.8 Hz), normal walk (1.8–2.2 Hz), brisk walk (2.2–2.7 Hz) and fast walk (greater than 2.7 Hz).

Considering the normal walk for example, if the vertical force function of one foot is defined as $F_n[t]$, and the period and foot contact time are T_n and T_{nc} (Fig. 4), respectively, then this function has the following property:

$$F_n[t] = \begin{cases} 0, & t<0 \text{ or } t>T_{nc}, \\ F_n[t], & 0 \leqslant t \leqslant T_{nc}. \end{cases} \tag{2}$$

The continuous vertical force function $F_{nv}(t)$ and lateral force function $F_{nl}(t)$ can therefore be expressed according to the pacing frequency f_p or load period T_p ($T_p = 1/f_p$).

$$F_{nv}(t) = \sum_{k=0}^{\infty} F_n[\alpha(t - kT_p)], \tag{3}$$

$$F_{nl}(t) = \sum_{k=0}^{\infty} \{F_n[\alpha(t - 2kT_p)] - F_n[\alpha(t - (2k+1)T_p)]\}, \tag{4}$$

$$\alpha = T_n/T_p \quad \text{or} \quad \alpha = f_p/f_n, \quad \left(1.8 \text{ Hz} \leqslant f_p < 2.2 \text{ Hz}\right), \tag{5}$$

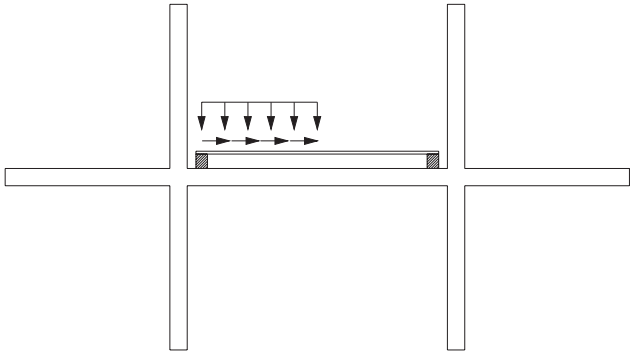

Fig. 5. Eccentric loads on bridge deck.

where α is a time factor, f_n and T_n are the pacing frequency and period ($f_n = 1/T_n$) shown in Fig. 4 for normal walk.

According to the assumptions, the walking dynamic load will consist of three parts: vertical dynamic force $q_{nv}(t)$, lateral dynamic force $q_{nl}(t)$ and vertical static force $q_{sv}(t)$. In numerical analysis, the static load is modelled as ramp load in order to reduce the fluctuation of dynamic response at the beginning of time history analysis. Therefore the walking loads for normal walk can be modelled as

$$q_{nv}(t) = 210F_{nv}(t)\ (\mathrm{N/m^2}), \tag{6a}$$

$$q_{nl}(t) = 8.4F_{nl}(t)\ (\mathrm{N/m^2}), \tag{6b}$$

$$q_{sv}(t) = \begin{cases} 840t/(10\alpha)\ (\mathrm{N/m^2}), & 0 < t < 10\alpha, \\ 840\ (\mathrm{N/m^2}), & t \geqslant 10\alpha. \end{cases} \tag{6c}$$

The loads caused by the other walking activities with other pacing frequencies can be similarly defined by following the same procedure.

To make the analysis simple, the pedestrians are assumed to walk eccentrically cross the footbridge, and hence the walking dynamic loads are distributed only on half the width of the deck (Fig. 5) along the whole bridge span length.

4. Natural frequencies and vibration modes

Natural frequencies and corresponding vibration modes are important dynamic properties and have significant effect on the dynamic performance of structures. Suspension bridges always have four main types of vibration modes: lateral, torsional, vertical and longitudinal modes. A suspension footbridge (with or without pre-tensioned reverse profiled cables) with shallow cable sag will also have these four types of vibration modes. However, numerical results [13] show that the lateral modes and torsional modes do not always appear as pure lateral or torsional vibration modes. Often, they are combined together and form two types of coupled vibration modes: coupled lateral–torsional modes (L_mT_n) and coupled torsional–lateral modes (T_mL_n), where L and T represent lateral and torsional modes, respectively and m and n are the number of half-waves. Coupled lateral–torsional vibration modes (Fig. 6) are dominated by the lateral vibration modes in conjunction with the torsional vibration. When the footbridge structure vibrates with a coupled lateral–torsional mode, the movement of the deck appears as if it has lateral movement and sways about a point above the deck. While coupled torsional–lateral modes (Fig. 7) are dominated by torsional vibration modes, and the deck has lateral movement and sways about a point underneath the bridge deck. Most vertical vibration modes appear as pure vertical modes, without corresponding lateral or torsional components. The longitudinal modes are sensitive to the connection between the adjacent bridge frames and disappear from the first 20 frequencies when pre-tensions are introduced.

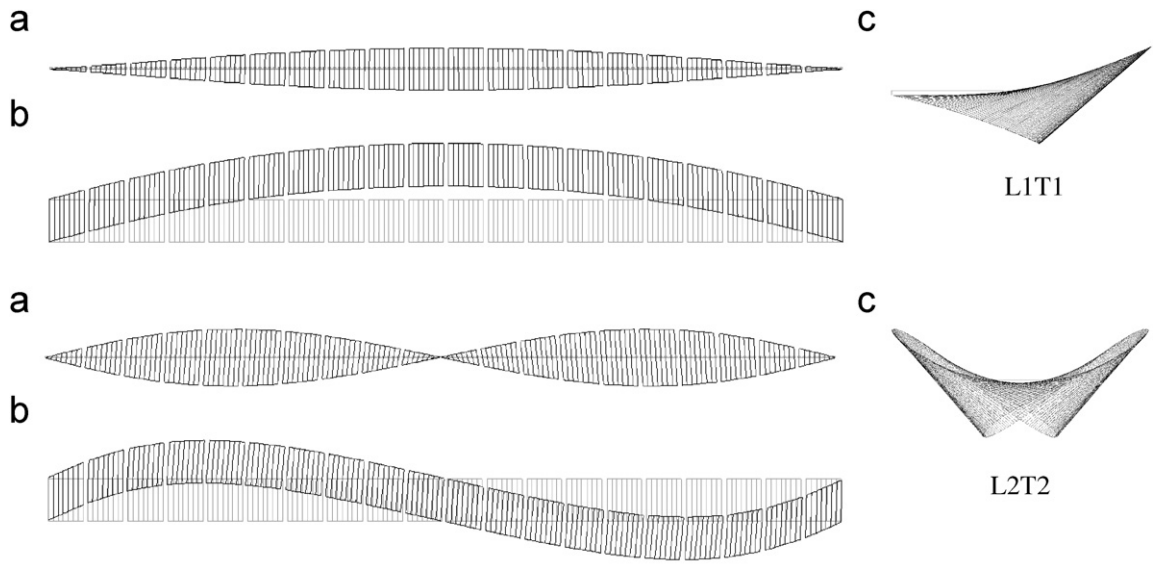

Fig. 6. Coupled lateral–torsional vibration modes: (a) elevation; (b) top view; (c) end view.

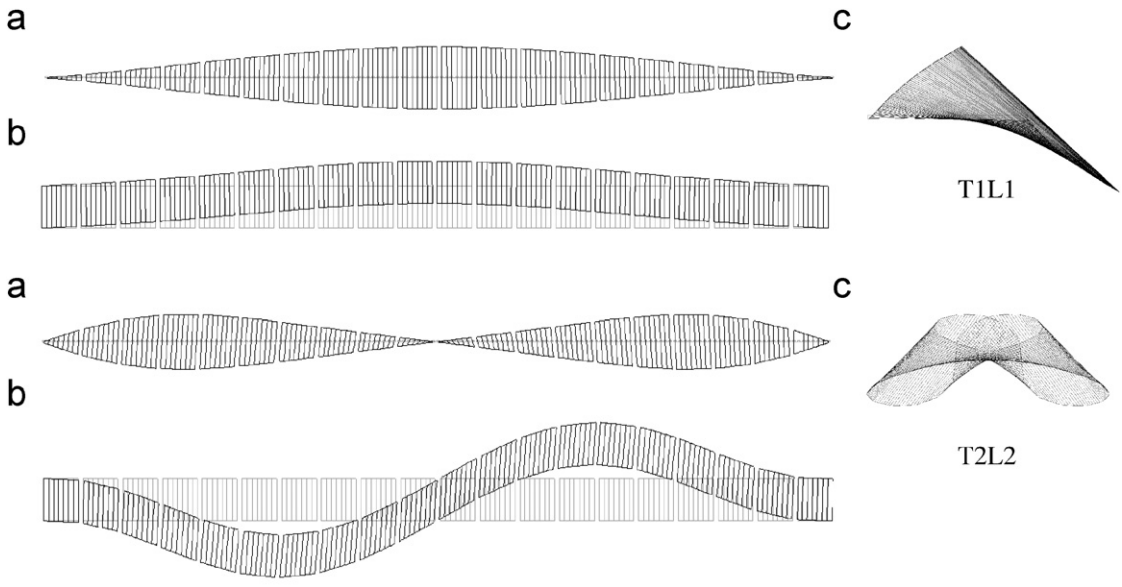

Fig. 7. Coupled torsional–lateral vibration modes: (a) elevation; (b) top view; (c) end view.

For slender footbridges, vibration at low frequency is more important than that at high frequency, as the fundamental natural frequencies in lateral direction are always low. Vibration modes with low natural frequencies can also be excited by crowd of walking pedestrians, even when the natural frequencies are out of the range of normal walk. For example, the lowest frequency of the lateral mode excited on the Millennium Bridge in London is about 0.48 Hz. This frequency coincides with a pacing frequency of 0.96 Hz and the frequency range of normal walk is supposed to vary from 1.6 to 2.4 Hz [1].

In order to illustrate the dynamic behaviour of slender footbridges with coupled vibration modes under walking dynamic loads, the natural frequency corresponding to the first coupled lateral–torsional mode of the

footbridge model A and bridge model B is set to be 0.75 Hz by introducing different tension forces in the reverse profiled cables. Table 1 shows some of the dynamic properties with relative structural parameters. Here the longitudinal modes are not listed. These bridge models have a span length of 80 m, cable sags of 1.8 m and cable diameters of 120 mm. In this table, the mass density M is obtained by dividing the total structural mass by the span length (80 m) and deck width (4 m), and the tension force T_1, T_2 and T_3 are the maximum tension forces at the end segment of the top supporting cables, reverse profiled bottom and side cables, respectively. From this table, it can be seen that when the natural frequency of the first coupled lateral–torsional mode (L_1T_1) is set to be the same, the other frequencies of the bridge model B are much smaller than those of bridge model A. This is because the lateral stiffness of the bridge model B has been improved by the side reverse profiled cables and the tension forces in the top and bottom cables required for the same fundamental natural frequency are smaller even though the mass density has increased.

Since bridge model C can be looked upon as an improved model from bridge model A, its pre-tension force in the reverse profiled bottom cables is kept as the same as that in bridge model A, while the tension force in the top supporting cables increases due to the increase of structural weight after the side legs and reverse profiled side cables have been added. As a result, the natural frequencies corresponding to the coupled lateral–torsional modes are higher than those of bridge model A (despite a small increase in structural weight), as the lateral stiffness has been improved by the pre-tensioned side cables. It is also found that the frequencies of coupled torsional–lateral modes and the first vertical mode decrease slightly while those corresponding to the higher vertical modes increase a little. This phenomenon implies that the reverse profiled side cables have only slight effect on the vertical and torsional stiffness. Comparing bridge models C and B, the natural frequencies of bridge model C are much higher than those of bridge model B. This is because the tension forces in the cable system of bridge model C are much greater than those of bridge model B, though they have the same cable configuration and mass density.

Table 1
Vibration properties of different bridge models

Bridge model	A	B	C
Mass density M (kg/m^2)	363.80	465.84	465.84
Cable tension			
T_1 (N)	6,987,428	5,536,132	7,901,332
T_2 (N)	3,722,268	1,356,765	3,722,863
T_3 (N)	—	1,110,712	3,339,126
Coupled lateral–torsional			
L_1T_1	0.7500	0.7500	0.9320
L_2T_2	1.4585	1.0980	1.5714
L_3T_3	2.1634	1.5602	2.2925
L_4T_4	2.8656	2.0340	3.0196
L_5T_5	3.5654	2.5246	3.7532
L_6T_6	4.2572	3.0111	4.4778
Coupled torsional–lateral			
T_1L_1	1.1949	0.8982	1.1184
T_2L_2	1.8718	1.4158	1.8613
T_3L_3	2.7238	2.0593	2.7181
T_4L_4	3.5793	2.7023	3.5773
Vertical			
V_1	1.0943	0.9062	1.0585
V_2	1.5151	1.1633	1.5829
V_3	2.2866	1.7597	2.3818
V_4	3.0239	2.3203	3.1551
V_5	3.7785	2.8998	3.9383

5. Resonant vibration under eccentric walking dynamic loads

When crossing a bridge which is vibrating at a frequency within the range of walking rates, pedestrians trend to change their pacing frequencies to move in harmony with the bridge vibration. This mechanism leads to large amplitude synchronous vibration. In other words, the bridge structure resonates at the vibration mode excited by the walking pedestrians. In general, when crowd walking dynamic loads are distributed uniformly on the entire bridge deck, the one half-wave coupled lateral–torsional mode (L_1T_1) and one half-wave vertical mode (V_1) are easy to be excited while the one half-wave coupled torsional–lateral mode (T_1L_1) is not. However, when the loads are distributed uniformly only on the half-width of the deck along the whole bridge length, all the one half-wave modes can possibly be excited.

To illustrate the dynamic response, the lateral and vertical deflections of the intersection point of the cross member and bridge legs (Point A in Fig. 8) are selected from the middle bridge frame and shown in the following figures and tables, as the maximum dynamic deflections occur at this location for the one half-wave vibration modes. In the following numerical analysis, the damping ratios for the first two vibration modes (such as L_1T_1 and L_2T_2, or V_1 and V_2, and so on) are assumed to be 0.01.

5.1. Resonant vibration of bridge model A

Footbridge structures vibrate at a frequency coinciding with the pacing frequency of walking pedestrians. When this pacing frequency coincides with one of the natural frequencies of the footbridge, the bridge structure is supposed to resonate with the corresponding vibration modes.

Fig. 9 shows the lateral and vertical deflections when pedestrians walk across the footbridge at the pacing frequency of 1.5 Hz. It can be seen that the footbridge resonates in the lateral direction as the frequency of lateral dynamic force generated by the walking pedestrians coincides with the natural frequency of the footbridge structure; while in the vertical direction, the footbridge vibrates with small amplitude as resonant vertical vibration is not expected at this pacing frequency. However, the vertical deflection is contributed by three parts: static deflection under static vertical force, dynamic deflection induced by the dynamic vertical force and dynamic deflection caused by the resonant lateral vibration [14].

Fig. 10 shows the dynamic response when the vertical mode V_1 is excited by pedestrians walking at the pacing frequency of 1.0943 Hz. It can be seen that the footbridge resonates in the vertical direction with large amplitude, and the lateral vibration consists of two parts: one caused by the lateral dynamic force and the other induced by the eccentric vertical dynamic force. However, it is found that the vertical dynamic force has only small contribution to the lateral vibration although eccentric static vertical load can cause lateral deflection [9]. It seems the effect of eccentric vertical dynamic load on the lateral vibration is different from that of eccentric static vertical load, and the lateral vibration is mainly induced by the lateral dynamic force.

Fig. 11 shows the dynamic lateral and vertical deflections when pedestrians walk on the half-width of deck at the pacing frequency of 1.1949 Hz (the natural frequency of the first coupled torsional–lateral mode T_1L_1). Since the vibration mode T_1L_1 is predominately torsional mode and is asymmetric about the centre line of the bridge deck, it is not easy to be excited by crowd walking dynamic loads symmetrically distributed on the entire deck, but can be excited by eccentric loads. When the footbridge structure resonates in this mode, it is found that both the lateral and vertical deflections have large amplitudes. The lateral vibration is mainly

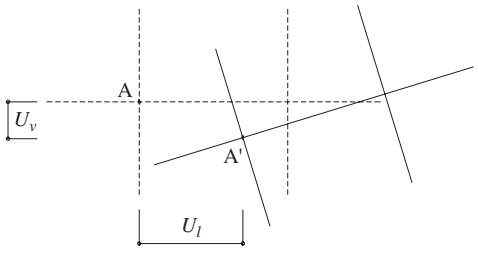

Fig. 8. Deflections and deformed bridge frame.

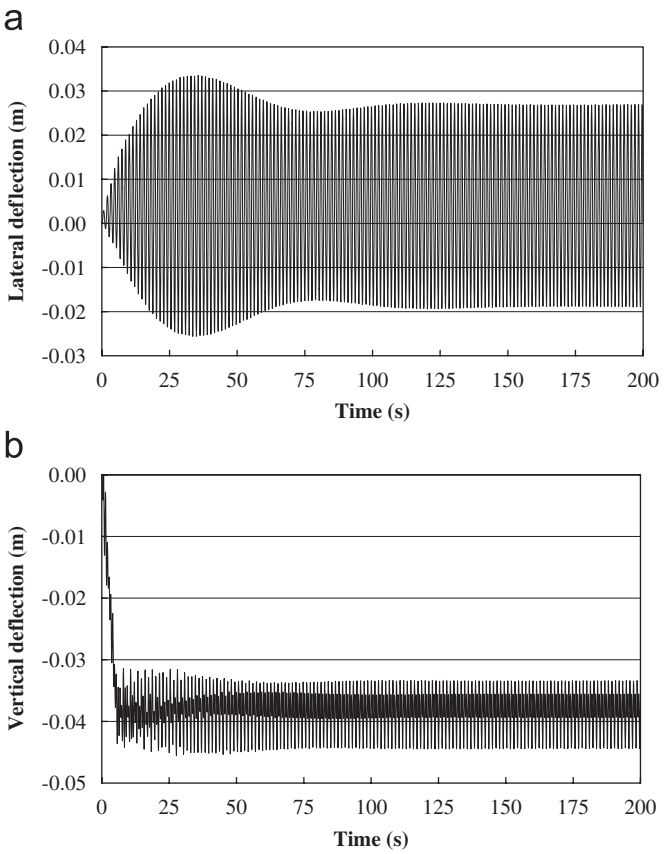

Fig. 9. Dynamic deflections of bridge model A under eccentric walking loads at pacing frequency of 1.5 Hz: (a) lateral deflection; (b) vertical deflection.

caused by the eccentric vertical dynamic force and enhanced by the lateral dynamic force. It can be seen that the lateral vibration has large constant amplitude but its mean value increases almost linearly with time, and it seems that the lateral deflection is contributed by both the vertical dynamic force and lateral dynamic force. It is found that the vertical deflection also has increasing mean value although this increase is very small. The increasing mean values of vibration in lateral and vertical direction are probably caused by the static load and/or the non-linearity of geometry.

Table 2 shows the statistics of steady dynamic deflections of an intersection point (Point A in Fig. 8) at the middle bridge frame (the same in the following tables) when pedestrians walk on half the width of deck at different pacing frequencies. The maximum and minimum deflections for the entire vibration are not listed and discussed as they are affected by the initial conditions. In this table, the lateral deflection U_l and vertical one U_v denote the components of the general deflection U, and this also applies for the other quantities in this and following tables. Here the static deflections (U_{static}) are produced by the quasi-static dynamic vertical force (defined by Eq. (6a)) as this dynamic force is the main cause of excitation when the crowd walking dynamic loads are distributed on the half-width of the bridge deck. Here and in the following tables, the maximum and minimum steady deflections (U_{stdmax} and U_{stdmin}) are the maximum and minimum peak values of the steady vibrations within a period of 15 s after the vibrations become steady. While for the vibrations with changing mean values, the maximum and minimum steady deflections are chosen from a typical periodic steady vibration cycle. The steady dynamic amplitude A_{ustd} and mean value M_{ustd} of lateral deflection are calculated based on their maximum value U_{stdmax} and minimum one U_{stdmin}:

$$A_{\text{ustd}} = \left|(U_{\text{stdmax}} - U_{\text{stdmin}})/2\right|, \tag{7}$$

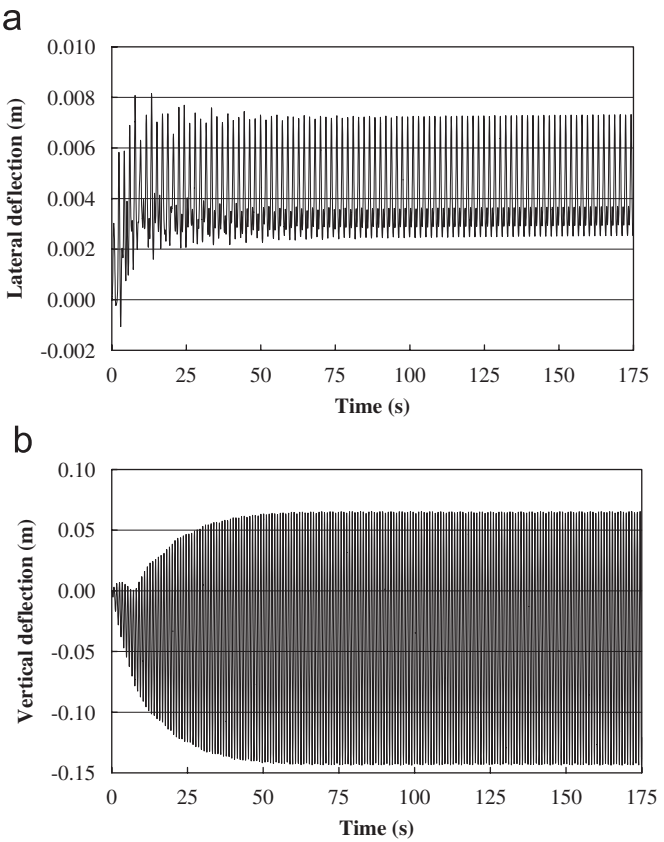

Fig. 10. Dynamic deflections of bridge model A under eccentric walking loads at pacing frequency of 1.0943 Hz: (a) lateral deflection; (b) vertical deflection.

$$M_{\text{ustd}} = (U_{\text{stdmax}} + U_{\text{stdmin}})/2. \tag{8}$$

The dynamic amplification factor (DAF) of deflections DAF_{ustd} is defined as

$$\text{DAF}_{\text{ustd}} = \left|A_{\text{ustd}}/U_{\text{static}}\right|. \tag{9}$$

From this table, it can be seen that large amplitude lateral vibration can be caused when the coupled vibration modes are excited by pedestrians walking across the footbridge on half-width of the deck. Resonant vibration with the coupled lateral–torsional mode is the main reason of excessive lateral vibration. However, resonant vertical vibration excited by vertical dynamic load does not cause large amplitude lateral vibration although eccentric vertical load incurs lateral deflection.

5.2. Resonant vibration of bridge model B

When the pre-tensioned side cables are introduced in the footbridge (bridge model B), the lateral stiffness can be improved, while the vertical stiffness is reduced when the same fundamental natural frequency in the lateral direction is required to compare the dynamic performance of footbridges with different cable configurations. This phenomenon has been shown in Table 1 and discussed previously. Due to this reason, the vibration properties are affected by the pre-tensioned side cables and hence the dynamic performance is influenced.

Table 3 shows the statistics of the steady dynamic deflections when pedestrians walk along the half-width of bridge deck with different pacing frequencies. When the first coupled lateral–torsional mode L_1T_1 is excited by pedestrians walking at the pacing frequency of 1.5 Hz, it is found that the lateral and vertical vibrations are

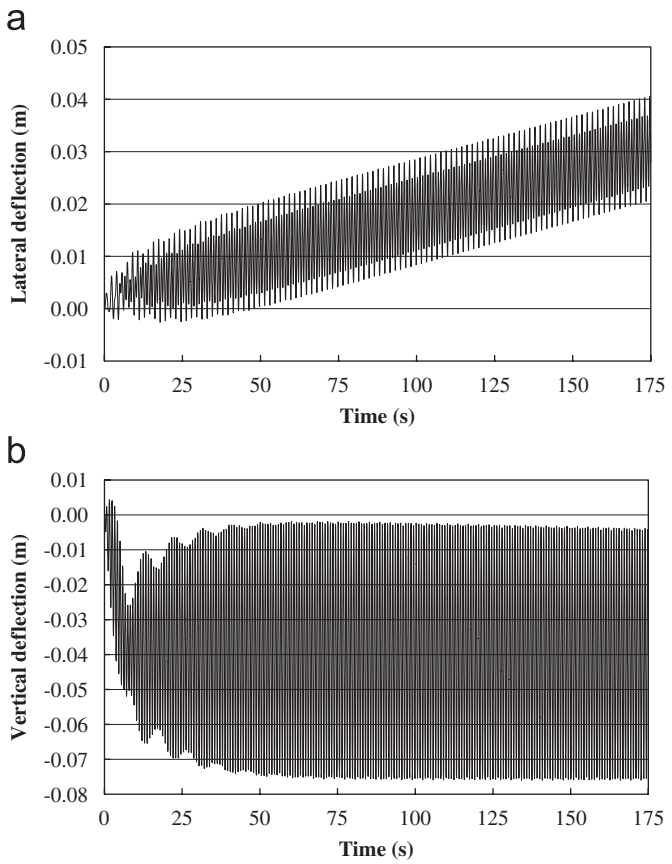

Fig. 11. Dynamic deflections of bridge model A under eccentric walking loads at pacing frequency of 1.1949 Hz: (a) lateral deflection; (b) vertical deflection.

Table 2
Dynamic deflections of bridge model A under eccentric walking dynamic loads

Bridge parameter		$L = 80$ m; $F_1 = F_2 = 1.8$ m; $D_1 = D_2 = 120$ mm					
Bridge model		A		A		A	
Vibration mode excited		L_1T_1		V_1		T_1L_1	
Pacing frequency	f_p (Hz)	1.5000		1.0943		1.1949	
Damping ratio		0.010		0.010		0.010	
Displacement	U	U_l	U_v	U_l	U_v	U_l	U_v
Static displacement	U_{static} (m)	0.00078	−0.00962	0.00078	−0.00962	0.00078	−0.00962
Steady vibration	U_{stdmax} (m)	0.02700	−0.03338	0.00733	0.06541	0.04030	−0.00370
	U_{stdmin} (m)	−0.01895	−0.04441	0.00252	−0.14366	0.02021	−0.07600
	A_{ustd} (m)	0.02297	0.00552	0.00240	0.10454	0.01004	0.03615
	M_{ustd} (m)	0.00403	−0.03889	0.00493	−0.03913	0.03025	−0.03985
	DAF_{ustd}	29.4	0.6	3.1	10.9	12.8	3.8

similar to those of bridge model A, but the amplitude and DAF of the lateral deflection are much smaller. The amplitude of the vertical deflection also decreases slightly while the mean value increases significantly, as the result of decrease of vertical stiffness. However, when the vertical mode V_1 and coupled mode T_1L_1 are excited, the footbridge structure experiences large vibrations in both lateral and vertical directions. Figs. 12

Table 3
Dynamic deflections of bridge model B under eccentric walking dynamic loads

Bridge parameter		$L = 80$ m; $F_1 = F_2 = F_3 = 1.8$ m; $D_1 = D_2 = D_3 = 120$ mm					
Bridge model		B		B		B	
Vibration mode excited		L_1T_1		V_1		T_1L_1	
Pacing frequency	f_p (Hz)	1.5000		0.9062		0.8982	
Damping ratio		0.010		0.010		0.010	
Displacement	U	U_l	U_v	U_l	U_v	U_l	U_v
Static displacement	U_{static} (m)	0.00078	−0.01080	0.00078	−0.01080	0.00078	−0.01080
Steady vibration	U_{stdmax} (m)	0.01399	−0.03827	0.04300	0.09294	0.02183	0.07244
	U_{stdmin} (m)	−0.00538	−0.04886	−0.01190	−0.17985	−0.00704	−0.15884
	A_{ustd} (m)	0.00969	0.00530	0.02745	0.13639	0.01444	0.11564
	M_{ustd} (m)	0.00430	−0.04357	0.01555	−0.04346	0.00740	−0.04320
	DAF_{ustd}	12.4	0.5	35.1	12.6	18.4	10.7

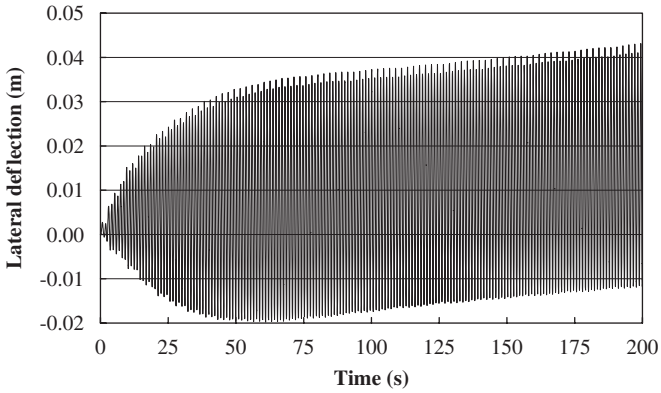

Fig. 12. Lateral deflections of bridge model B under eccentric walking loads at pacing frequency of 0.9062 Hz.

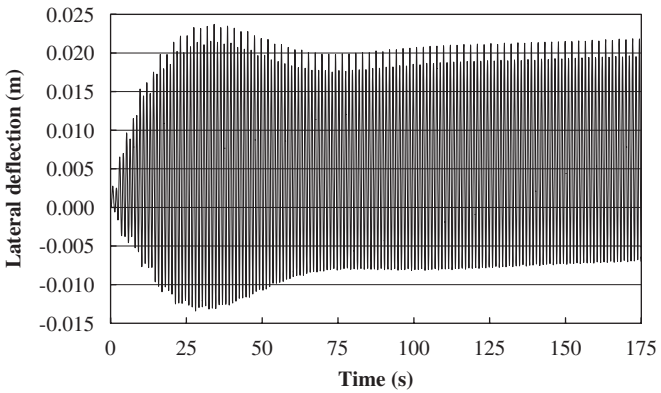

Fig. 13. Lateral deflections of bridge model B under eccentric walking loads at pacing frequency of 0.8982 Hz.

and 13 show the lateral deflections under eccentric walking loads with different pacing frequencies and it is found that both these lateral deflections have increasing mean values and the lateral deflections are mainly caused by the vertical dynamic forces. The similarity of resonant vibration feature under eccentric dynamic loads in the modes V_1 and T_1L_1 is probably due to their close natural frequencies.

Table 4
Dynamic deflections of bridge model C under eccentric walking dynamic loads

Bridge parameter		$L = 80$ m; $F_1 = F_2 = F_3 = 1.8$ m; $D_1 = D_2 = D_3 = 120$ mm					
Bridge model		C		C		C	
Vibration mode excited		L_1T_1		V_1		T_1L_1	
Pacing frequency	f_p (Hz)	1.8640		1.0585		1.1184	
Damping ratio		0.010		0.010		0.010	
Displacement	U	U_l	U_v	U_l	U_v	U_l	U_v
Static displacement	U_{static} (m)	0.00034	−0.00773	0.00034	−0.00773	0.00034	−0.00773
Steady vibration	U_{stdmax} (m)	0.01111	−0.02529	0.00530	0.05503	0.02370	−0.00737
	U_{stdmin} (m)	−0.00786	−0.03440	−0.00107	−0.11715	−0.00256	−0.05612
	A_{ustd} (m)	0.00948	0.00455	0.00319	0.08609	0.01313	0.02437
	M_{ustd} (m)	0.00162	−0.02985	0.00211	−0.03106	0.01057	−0.03175
	DAF_{ustd}	28.2	0.6	9.5	11.1	39.1	3.2

5.3. Resonant vibration of bridge model C

As the bridge model is developed from bridge model A, the lateral stiffness is significantly improved by the pre-tensioned side cables while the vertical stiffness just changes slightly. This can be seen from the change of natural frequencies in Table 1 and the static deflections in Table 4. Table 4 shows the statistics of the steady vibrations when different vibration modes are excited by pedestrians walking eccentrically on the half-width of the deck at different pacing frequencies. It is found that the dynamic performance of bridge model C is similar to that of bridge model A. When the footbridge resonates in the coupled mode L_1T_1, the lateral vibration is mainly induced by the lateral dynamic force. Though the dynamic amplitude is much smaller than that of bridge model A, the DAF is much larger as the static deflection is smaller. When the footbridge resonates in the vertical mode V_1, the lateral vibration is mainly induced by the lateral dynamic force. While when the coupled mode T_1L_1 is excited, it is found that the lateral vibration is mainly caused by the eccentric vertical dynamic force, but its amplitude is much larger although the amplitude of vertical vibration decreases. This phenomenon indicates that the vibration in coupled mode is much complex than those in pure lateral or torsional modes, and it is not only affected by the natural frequency and mode shape, but affected by other factor such as the ratio of lateral component to the vertical one. For example, it is found that the ratio of lateral component to vertical one of coupled mode T_1L_1 is 0.12238 for bridge model A, 0.47099 for bridge model B and 0.27587 for bridge model C. It seems that higher amplitude lateral vibration would accompany the vertical one for a coupled torsional–lateral mode. This is probably one reason why large amplitude lateral vibration still occurs even when the structural stiffness has been improved and the amplitude of vertical vibration has been reduced.

6. Conclusion and discussion

Suspension footbridge is an important and popular structural form of modern footbridges. Due to the new technology and application of light weight and high strength materials, modern suspension footbridges are often designed and constructed slender and flexible with low mass and low stiffness. Some can also be designed as ribbon bridges with shallow cable profiles to satisfy different aesthetic requirements. However, such slender footbridges are always prone to vibration induced by pedestrians and have risk of suffering serious vibration serviceability problems.

In this conceptual study, a suspension footbridge model with reverse profiled cables is proposed to investigate the vibration characteristics of shallow suspension pedestrian bridge structures. This paper concerns the vibration of slender suspension footbridges under eccentrically distributed walking dynamic loads. It is found that large amplitude lateral vibration is mainly caused by the resonant vibration in coupled vibration modes. When the first coupled lateral–torsional mode is excited, the large amplitude lateral vibration is induced by the lateral dynamic force; while when the first coupled torsional–lateral mode is excited, the

excessive lateral vibration with increasing mean value is mainly caused by the vertical dynamic force and enhanced by the lateral dynamic force. When the first vertical mode is excited, the amplitude of lateral vibration is quite small and it is mainly caused lateral dynamic force.

It is known that pedestrians are much more sensitive to low-frequency lateral vibration when walking or running than to the vertical vibration. The acceptable amplitudes of acceleration and deflection in vertical direction are five times of those in the lateral direction [1]. On the other hand, suspension footbridges always have much weaker structural stiffness in the lateral direction than in the vertical direction, and they are in danger of suffering excessive lateral vibrations. Therefore, vibration control in the lateral direction is important for the serviceability of slender suspension footbridges. In real footbridge situation, the resonant lateral vibration induced by synchronous lateral excitation is the most important source for lateral vibration serviceability problem as it is quite normal that pedestrians walk across a footbridge on whole bridge deck and the lateral or coupled lateral–torsional modes are easily excited. However, it is also common that there are always eccentric loads existing on the bridge deck due to different reasons such as different weights of people or pedestrians walking eccentrically on the deck. Since this lateral vibration is induced by eccentrically distributed vertical load, it is independent of the phases of footfalls and may make more pedestrians be aware of the lateral vibration and hence trigger the synchronous lateral excitation. This can happen more easily on slender footbridges which have nearly integer frequency ratios [15] between vertical and lateral natural frequencies, as it is probably convenient for pedestrians to adjust their footfalls to the pacing frequencies coinciding with the bridge vibrating at its lateral natural frequency.

It seems that for slender footbridge structures, it is important to improve the lateral stiffness and hence to reduce the level of lateral vibration caused by synchronous lateral excitation. It is also important to suppress the lateral vibration induced by eccentric loads as this vibration could also be a source for lateral vibration serviceability problem, and it also provides an opportunity to trigger synchronous lateral excitation.

References

[1] H. Bachmann, "Lively" footbridges—a real challenge, *Proceedings of the International Conference on the Design and Dynamic Behaviour of Footbridges*, Paris, France, November 20–22, 2002.
[2] A.-I. Nakamura, Model for lateral excitation of footbridges by synchronous walking, *Journal of Structural Engineering* 130 (1) (2004) 32–37.
[3] M. Willford, Dynamic actions and reactions of pedestrians, *Proceedings of the International Conference on the Design and Dynamic Behaviour of Footbridges*, Paris, France, November 20–22, 2002.
[4] P. Dallard, T. Fitzpartrick, A. Low, R.R. Smith, M. Willford, M. Roche, London Millennium Bridge: pedestrian-induced lateral vibration, *Journal of Bridge Engineering* 6 (6) (2001) 412–416.
[5] S.-I. Nakamura, Y. Fujino, Lateral vibration on a pedestrian cable-stayed bridge, *Structural Engineering International: Journal of the International Association for Bridge and Structural Engineering (IABSE)* 12 (4) (2002) 295–300.
[6] S. Zivanovic, A. Pavic, P. Reynolds, Vibration serviceability of footbridges under human-induced excitation: a literature review, *Journal of Sound and Vibration* 279 (1–2) (2005) 1–74.
[7] T. Ji, B.R. Ellis, A.J. Bell, Horizontal movements of frame structures induced by vertical loads, *Proceedings of the Institution of Civil Engineers, Structures and Buildings* 156 (2) (2003) 141–150.
[8] H. Xia, N. Zhang, Dynamic analysis of railway bridge under high-speed trains, *Computers and Structures* 83 (23–24) (2005) 1891–1901.
[9] M.-H. Huang, D.P. Thambiratnam, N.J. Perera, Load deformation characteristics of shallow suspension footbridge with reverse profiled pre-tensioned cables, *Structural Engineering and Mechanics* 21 (4) (2005) 375–392.
[10] CSI, *CSI Analysis Reference Manual for SAP2000, ETABS, and SAFE*, Computers and Structures, Inc., California, USA, 2004.
[11] J.E. Wheeler, Prediction and control of pedestrian induced vibration in footbridges, *Journal of the Structural Division* 108 (ST9) (1982) 2045–2065.
[12] Y. Fujino, B.M. Pacheco, S.-I. Nakamura, P. Warnitchai, Synchronization of human walking observed during lateral vibration of a congested pedestrian bridge, *Earthquake Engineering and Structural Dynamics* 22 (9) (1993) 741–758.
[13] M.-H. Huang, D.P. Thambiratnam, N.J. Perera, Vibration characteristics of shallow suspension bridge with pre-tensioned cables, *Engineering Structures* 27 (8) (2005) 1220–1233.
[14] M.-H. Huang, D.P. Thambiratnam, N.J. Perera, Resonant vibration of shallow suspension footbridges, *Proceedings of Institute of Civil Engineering: Bridge Engineering* 158 (BE4) (2005) 201–209.
[15] A.N. Blekherman, Swaying of pedestrian bridges, *Journal of Bridge Engineering* 10 (2) (2005) 142–150.